Adsorption of fullerene nC[60] on activated sludge: Kinetics, equilibrium and influencing factors

AUTHOR(S):

Yang, Yongkui; Nakada, Norihide; Tanaka, Hiroaki

Adsorption of fullerene nC_{60} on activated sludge: kinetics, equilibrium and influencing factors

Yongkui Yang, Norihide Nakada, Hiroaki Tanaka*

Research Center for Environmental Quality Management, Kyoto University, 1-2 Yumihama, Otsu, Shiga 520-0811, Japan

Email:
ykyang@biwa.eqc.kyoto-u.ac.jp
nakada.norihide.8w@kyoto-u.ac.jp
htanaka@biwa.eqc.kyoto-u.ac.jp

*Corresponding author:
Hiroaki Tanaka
Research Center for Environmental Quality Management, Kyoto University
Tel: +81 77 527 6222
Fax: +81 77 524 9869
Email: htanaka@biwa.eqc.kyoto-u.ac.jp

Abstract

The increasing production and use of fullerene C_{60} nanomaterials raises concerns about environmental risks and human health. However, the materials' behavior and fate during wastewater treatment are still unclear. We investigated the adsorption of aqueous nanoscale fullerene (nC_{60}) on activated sludge by analysis of adsorption kinetics and equilibrium. The adsorption process closely followed the pseudo-second-order kinetics model, and the adsorption isotherm was well described by the Freundlich model. The adsorption process depended strongly on the activated sludge concentration and pH, but there was no significant effect by the temperature and low ionic strength. The dissolved organic matter in wastewater could obviously inhibit the adsorption process. At mixed liquor suspended solids concentrations of 1000 and 2000 mg/L after 1 h mixing, nC_{60} removal by adsorption reached 47% and 74%, respectively. Thus, adsorption could play an important role in the fate of nC_{60} during conventional biological wastewater treatment. The analysis of factors influencing the adsorption amounts indicated that the nC_{60} adsorption behavior on activated sludge was affected by the combined forces of the hydrophobic attraction, electrostatic repulsion and steric interaction.

Keywords: Fullerene nC_{60}; Activated sludge; Adsorption; Model; Influencing factors

1. Introduction

Fullerene C_{60} consists of 60 carbon atoms arranged in 20 hexagons and 12 pentagons and forming a hollow sphere about 1 nm in diameter [1]. Being chemically and thermally stable, an excellent electron acceptor, and a radical scavenger, and having special optical properties, it is attracting commercial and scientific interest [2]. Fullerene C_{60} and other carbon-based nanomaterials are the second most nanomaterials used in consumer products available in 2011 [3]. Their growing production and use will inevitably result in the entry of fullerenes into the environment, raising concerns about environmental risks and human health [4–6].

The extremely low solubility (7.96 ng/L) and high hydrophobicity (log K_{ow} 6.67) of C_{60} molecules assumed little chance of transport into aquatic environments and consequent limited risk to humans [7]. However, recent studies showed C_{60} molecules can form stable nanoscale colloidal aggregates (nC_{60}) in water with concentrations at mg/L level via solvent exchange and/or sonication treatment [8–11], as well as the environmental extended mixing [12–15]. C_{60} has been detected in the commercial cosmetics ranging from 0.04 to 1.1 μg/g [16] and <0.005% (w/w) [17] which suggesting the potential pathway of C_{60} from consumer products to the wastewater streams. Farré et al. [18] firstly reported the nC_{60} concentration up to ~20 μg/L in the suspended solids of the wastewater effluents. However, very few studies have examined the fate of nC_{60} during wastewater treatment. No biodegradation was found in either aerobic [19] or anaerobic systems [20]. Wang et al. [21] reported a high removal of 83–97% for nC_{60} during the sequencing batch reactor wastewater treatment process. However, the information is very limited on the adsorption kinetic, equilibrium, and the factors influencing the nC_{60} adsorption on activated sludge which is essential to evaluate the fate, and to improve the removal of nC_{60} during the wastewater treatment.

The objective of this study was to investigate the behavior and mechanism of nC_{60} adsorption on activated sludge. We investigated the adsorption kinetics and equilibrium of nC_{60}, conducted adsorption modeling to determine the adsorption mechanism, and studied the effects of mixed liquor suspended solids (MLSS), temperature, ionic strength, pH, and wastewater dissolved organic matter (DOM) on nC_{60} adsorption on activated sludge.

2. Materials and methods

2.1 Preparation of fullerene nC_{60} aqueous suspension

nC_{60} suspension was prepared according to the widely used toluene-based solvent exchange method [22–24] with minor modifications. Detailed procedure was described in our previous work [25].

2.2 Sampling and sample preparation

Activated sludge and three wastewater samples (primary effluent, aeration tank liquor and secondary effluent) were collected from a municipal wastewater treatment plant in Japan, which used a conventional biological wastewater treatment process with a hydraulic retention time of ~8 h, a sludge retention time of ~18 d, and an MLSS level of ~2570 mg/L. All the wastewater samples were filtered through a glass fiber filter (1.0 μm pore size; GF/B, Whatman, Germany) and adjusted to pH 7 with dilute NaOH or HCl solution. The activated sludge sample was washed in filtered primary effluent and centrifuged at 2000 ×*g* for 5 min. The pellet was washed and centrifuged twice more. After the last centrifugation, it was suspended in filtered primary effluent to an MLSS level of 6000 mg/L and stored at 4 °C. The liquid was diluted to the required MLSS level with filtered wastewater samples just before the adsorption experiments started. The activated sludge was not inactivated, because nC_{60} is not biodegradable [19,20,26].

2.3 Adsorption kinetics and isotherm experiments

For the kinetics and isotherm studies, 100-mL Erlenmeyer flasks containing 50 mL primary effluent at 1000 mg/L MLSS were agitated on a rotary shaker (125 rpm) at room temperature (25 °C). For the kinetics study, the initial nC_{60} concentrations were 0.100, 0.300, and 0.500 mg/L. Samples were collected at various time intervals and were centrifuged at 2000 ×*g* for 5 min, and the supernatant was collected (5 mL) for nC_{60} quantification. For the adsorption isotherm experiments, the initial nC_{60} concentrations were 0.050, 0.100, 0.200, 0.350, and 0.500 mg/L. From the results of the kinetics studies, we chose 12 h as the equilibrium time in the isotherm experiments. After the equilibrium time, the samples were collected and centrifuged as above. The nC_{60} in supernatant was extracted using toluene and then analyzed by a high-performance liquid chromatography (HPLC) system equipped with a UV/visible detector (Shimadzu, Japan), as described in Section 2.5. Reference samples without activated sludge were analyzed, so we could subtract nC_{60} losses such as by adsorption to glassware. Adsorption to activated sludge was calculated from the mass balance of the nC_{60} concentrations between the experimental and reference samples:

$$q_t = \frac{C_{(ref,\,t)} - C_{(exp,\,t)}}{MLSS} \quad (1)$$

where q_t is the nC_{60} adsorbed on the activated sludge at time t (mg/g), $C_{(ref,\,t)}$ is the nC_{60} concentration in the aqueous phase in reference samples at time t (mg/L), $C_{(exp,\,t)}$ is that in experimental samples at time t (mg/L), and MLSS is the mixed liquor suspended solids concentration in the flask (g/L).

2.4 Factors affecting the adsorption of nC_{60} on activated sludge

Batch experiments were conducted to study the effects of MLSS concentration, temperature, ionic strength, pH, and wastewater DOM on the nC_{60} adsorption on activated sludge (Table 1). Three wastewater samples (primary effluent, aeration tank liquor and secondary effluent) were used to study the DOM effect, while only primary effluent was used in all other experiments. Short contact time of 1 h was here determined to ensure approximate 50% of initial nC_{60} left after adsorption in order to increase the sensitivity which helps obtain a better investigation of the adsorption mechanism.

2.5 Quantification of nC_{60}

nC_{60} in supernatant was extracted by the liquid-liquid extraction method and measured by the HPLC-UV/visible system as reported [10,24] with a slight modification: specifically, NaCl was added to 5 mL of sample up to 1% by weight for nC_{60} destabilization, followed by 3 mL of toluene as extraction solvent. The mixture was agitated at 200 rpm for 30 min on the rotary shaker. The aqueous and toluene phases were then separated by centrifugation at 1000 $\times g$ for 5 min, and the toluene layer was collected for analysis. C_{60} in the toluene was quantified by the HPLC-UV/visible system (Shimadzu, Japan). C_{60} was separated in a triacontyl (C30) silica-gel column (250 mm×4.6 mm i.d. packed with 5-µm particles; Nomura Chemical, Japan) by isocratic elution at a flow rate of 1 mL/min in a mobile phase of acetonitrile and toluene (65:35, v/v) at 30 °C. C_{60} was quantified at 332 nm. The calibration curve was obtained by spiking varying amounts of nC_{60} aqueous suspensions in 5 mL of 1.0-µm-filtered wastewater. Preliminary results showed a recovery rate of > 90% with a very high correlation coefficient ($R^2 > 0.998$).

2.6 Other analysis

The dissolved organic carbon (DOC) concentration in wastewater samples was measured with a TOC analyzer (5000A, Shimadzu, Japan). The size of nC_{60} and activated sludge were determined using a dynamic light scattering Zetasizer (Nano ZS, Malvern, UK) and laser diffraction size analyzer (SALD-2100, Shimadzu, Japan), respectively. The electrophoretic mobility of nC_{60} and activated sludge were measured with the Zetasizer and used to calculate the zeta (ζ) potential by the Smoluchowski equation [27]. For the activated sludge, the specific surface area and relative hydrophobicity were measured by the methods of the Rhodamine B adsorption [28-30] and the adherence to hexadecane hydrocarbon [31,32], respectively. The mixed liquor volatile suspended solids (MLVSS) and mixed liquor suspended solids (MLSS) of activated sludge were determined according to the standard method [33].

149 # 3. Results and discussion

150 ## *3.1 Properties of nC_{60}, activated sludge and wastewater samples*

151 The intensity-weighted size distribution (Fig. S1 (a), Supplemental data) of the nC_{60}
152 suspension gave a hydrodynamic diameter of 138 nm with a polydispersity index of 0.095.
153 The ζ potential in Milli-Q water showed the nC_{60} suspension was negatively charged in the
154 range of pH studied and the absolute value decreased with the decrease in pH from 11 to 1
155 (Fig. S1 (b), Supplemental data). The activated sludge used in this study was characterized to
156 be 139.0 μm in size, –17.0 mV (in primary effluent) in ζ potential, 74.6% in relative
157 hydrophobicity, 11.5 m^2/g MLSS in specific surface area, and 78.5% in MLVSS/MLSS. And
158 three wastewater samples had a DOC concentration of 40.8, 5.3, and 4.1 mg/L for the primary
159 effluent, aeration tank liquor, and secondary effluent, respectively.

160 ## *3.2 Time profile of nC_{60} adsorption on activated sludge*

161 At a lower initial nC_{60} concentration, the adsorption of nC_{60} on the activated sludge (q_t)
162 reached equilibrium sooner (Fig. 1) because of the relative abundance of adsorption sites
163 available. At all initial concentrations tested, the adsorption reached equilibrium after 12 h, so
164 we used 12 h as the equilibrium time in the following adsorption isotherm experiments.

165 ## *3.3 Adsorption kinetics*

166 To understand the mechanism of adsorption, we fitted the pseudo-first-order and pseudo-
167 second-order models to the experimental data.

168 ### *3.3.1 Pseudo-first-order model*

169 The linear pseudo-first-order model is given as [34]:

170 $$\ln (q_e - q_t) = \ln q_e - k_1 t \quad (2)$$

171 where q_t (mg/g) and q_e (mg/g) are the amounts of nC_{60} adsorbed on activated sludge at time t
172 (h) and at equilibrium, respectively; and k_1 (1/h) is the rate constant of pseudo-first-order

adsorption. The q_e and k_1 can be determined from the slope and intercept by plotting $\ln(q_e - q_t)$ versus t.

3.3.2 Pseudo-second-order model

The linear pseudo-second-order model is given as [35]:

$$\frac{t}{q_t} = \frac{1}{k_2 q_e^2} + \frac{1}{q_e} t \quad (3)$$

where k_2 (g/(mg·h)) is the rate constant of pseudo-second-order adsorption. The q_e and k_2 can be determined from the slope and intercept by plotting t/q_t versus t.

3.3.3 Model results

The adsorption kinetics at different initial concentrations were fitted to Eqs.(2) and (3) (Fig. 2). The data fitted the second-order model much better than the first-order model. The model's correlation coefficient was > 0.99 and the calculated ($q_{e(cal)}$) values were very close to the observed ($q_{e(obs)}$) values (Table 2). Both facts indicate that the adsorption of nC_{60} on activated sludge was well fit by the second-order model, indicating that nC_{60} adsorption on activated sludge was affected by chemical process [36,37]. The interaction between the :OH on nC_{60} surface [38] and the functional groups on activated sludge might contribute to this chemical adsorption by forming hydrogen bond, which are intermediate in strength between van der Waals bond and covalent bond [39]. In addition, the rate constant (k_2) of the second-order model decreased with increasing initial nC_{60} concentration, showing the adsorption rate increased at higher nC_{60} concentration.

3.4 Adsorption isotherm

There are several adsorption isotherms for fitting the adsorption process based on different adsorption mechanisms. Among these, the Langmuir and Freundlich models are widely used for modeling the adsorption on activated sludge such as estrogens [40,41], dyes [42,43], and heavy metals [44]. Therefore, both isotherms were applied in this work.

3.4.1 Langmuir model

The Langmuir model assumes that the adsorption occurs on specific homogeneous sites of the adsorbent surface in a monolayer [45]. The linear form is given as:

$$\frac{C_e}{q_e} = \frac{1}{k_L q_m} + \frac{1}{q_m} C_e \quad (4)$$

where q_m (mg/g) is the maximum adsorption capacity of nC_{60} on activated sludge, C_e (mg/L) is the nC_{60} concentration in the aqueous phase at equilibrium, and k_L is the Langmuir constant (L/mg). The values of k_L and q_m can be determined from the intercept and slope by plotting C_e/q_e versus C_e (Fig. 3a).

The essential feature of the Langmuir isotherm can be expressed by the equilibrium parameter R_L, which indicates the favorability of the adsorption process. The values of R_L indicate the adsorption to be irreversible ($R_L = 0$), favorable ($0 < R_L < 1$), linear ($R_L = 1$) or unfavorable ($R_L > 1$) [46,47]:

$$R_L = \frac{1}{1 + k_L C_0} \quad (5)$$

where C_0 is the initial nC_{60} concentration in the aqueous phase (mg/L).

3.4.2 Freundlich model

The Freundlich model expresses the adsorption process on a heterogeneous surface with different binding energies [48]. The linear form is given as:

$$\ln q_e = \ln k_F + \frac{1}{n} \ln C_e \quad (6)$$

where k_F and n are Freundlich constants. And they can be determined from the intercept and slope by plotting $\ln q_e$ versus $\ln C_e$ (Fig. 3b).

3.4.3 Model results

The equilibrium parameter R_L was < 1, indicating that the adsorption process was favorable (Table 3). In addition, the value of n in the Freundlich model lay between 1 and 10, indicating the favorable adsorption of nC_{60} on activated sludge [49]. The correlation

coefficients showed that the Freundlich model better described the experimental data, implying that it is more suitable for modeling nC_{60} adsorption on activated sludge (Fig. 3b). This result indicated the nC_{60} adsorption occurred at multi-layer and on the heterogeneous surface of activated sludge [50-52].

3.5 Factors affecting the adsorption behavior of nC_{60} on activated sludge

3.5.1 Effect of MLSS concentration

The nC_{60} concentration in the aqueous phase decreased as the MLSS increased from 50 to 4000 mg/L (Fig. 4a). The decrease in concentration can be partially attributed to the increased surface area and availability of more adsorption sites, as also seen in the adsorption of dye on activated sludge [53]. At MLSS concentrations of 1000 and 2000 mg/L, which are common in conventional activated sludge treatment, the reduction of nC_{60} in the aqueous phase were 47% and 74%, respectively, indicating that adsorption on activated sludge played an important role in the removal of nC_{60} during activated sludge process. The strong correlation between the adsorption amounts and sludge concentrations (Fig. 4a), and proved hydrophobic surface of nC_{60} [54] indicated the attractive hydrophobic interaction affected the nC_{60} adsorption on activated sludge.

3.5.2 Effect of Temperature

The nC_{60} adsorption slightly increased from 46 to 60% with increasing temperature from 15 to 35 °C (Fig. 4b). However the increase was not significant according to the Analysis of Variance ($p > 0.05$) which indicated there was no obvious effect of temperature on the nC_{60} adsorption.

3.5.3 Effect of ionic strength

At an added ionic strength of ≤10 mM—in the range of common surface waters, domestic wastewater, and groundwaters—there was no significant effect on nC_{60} adsorption

(Fig. 5a). However, adsorption was decreased at 50 and 500 mM, levels of some industrial wastewaters or wastewater mixed with seawater. This result is opposite to the hypothesis that an increase in ionic strength would decrease the surface charge of activated sludge and nC_{60} and thus increase the adsorption on activated sludge. A higher ionic strength indeed decreased the negative charge of activated sludge (Fig. 6a), along with that of nC_{60} as reported in our previous work [55]. However, the increasing ionic strength also increased the concentration of dissolved organic carbon (DOC) in the supernatant (Fig. 6a). This result indicated that the nC_{60} could remain stable in solution and was prevented from adsorbing to activated sludge by coexisting DOM even with very low electrostatic repulsion at high ionic strength. And the effect of DOM on nC_{60} adsorption is discussed in detail in Section 3.5.5.

3.5.4 Effect of pH

nC_{60} adsorption on activated sludge was highly dependent on pH, increasing as the pH decreased (Fig. 5b). pH could affect both the adsorbate and the adsorbent through its effects on surface charge, protonation, and speciation [56,57]. The ζ potential of activated sludge in primary effluent was negative within the pH range studied, and the absolute values decreased as the pH decreased (Fig. 6b). Previous studies showed the change in ζ potential of nC_{60} in primary effluent as a function of pH was consistent with the activated sludge [55]. At lower pH, proton neutralization could decrease the surface charge of nC_{60} and activated sludge, decreasing electrostatic repulsion and consequently increasing nC_{60} adsorption on activated sludge. The results here indicated the role of electrostatic effect in the nC_{60} adsorption on activated sludge. Similar behavior was also observed on the adsorption of negative-charged perfluorooctane sulfonate [58] and anionic dye [57] on activated sludge. In addition, at pH 11, the DOC concentration obviously increased (Fig. 6b) which might enhance the stability of nC_{60} in water (discussed in Section 3.5.5). Therefore, both a stronger electrostatic repulsion force and an increasing stabilizing effect resulted in the lowest adsorption at pH 11.

3.5.5 Effect of wastewater DOM

nC_{60} adsorption on activated sludge increased by ~18% in secondary effluent compared to that in primary effluent (Fig. 5c), as the DOC concentration in sludge mixture decreased from 40.1 to 11.3 mg/L (Fig. 6c). This indicated the wastewater DOM could greatly inhibit the nC_{60} adsorption on activated sludge. Although no difference was observed in absolute ζ potential of nC_{60} in three wastewater samples (Fig. S1 (c), Supplemental data), that of activated sludge was much higher in primary effluent (Fig. 6c). This might result in the decrease in nC_{60} adsorption on activated sludge in primary effluent by increasing the electrostatic repulsion between nC_{60} and activated sludge. In addition, our previous study found the wastewater DOM could greatly inhibit the nC_{60} aggregation in water via the steric stabilization [55]. Kiser et al. [59] recently reported the cellular matter (proteins and other soluble organics) of activated sludge greatly reduced the removal of the nanoparticles (nC_{60}, Ag, Au, and polystyrene) from the aqueous solutions. Therefore, these results here showed the DOM in wastewater could inhibit the nC_{60} adsorption on activated sludge by both the electrostatic and steric effect.

4. Conclusions

This study examined the adsorption of nC_{60} on activated sludge by adsorption kinetics, and equilibrium. Adsorption reached equilibrium after 12 h at an MLSS level of 1000 mg/L at 25 °C. The process was well fit by the pseudo-second-order kinetic model and the Freundlich isotherm model.

pH greatly affected the adsorption process, decreasing the adsorption of nC_{60} from 86% at pH 3 to 26% at pH 11. At an ionic strength of 0 to10 mM, there was no significant effect on nC_{60} adsorption. Adsorption was obviously inhibited by coexisting dissolved organic matter in wastewater through electrostatic and steric stabilization effect. At MLSS levels of 1000 and 2000 mg/L, similar to the conditions in conventional activated sludge treatment, the adsorption reached 47% and 74%, demonstrating high removal efficiency. The analysis of factors influencing the adsorption amounts indicated that the nC_{60} adsorption behavior on activated sludge was affected by the combined forces of the hydrophobic attraction, electrostatic repulsion and steric interaction.

Acknowledgements

This research was partly supported by Grant-in-Aid for Scientific Research (B) from the Japan Society for the Promotion of Science (JSPS) and by the CREST project of the Japan Science and Technology (JST) organization.

References

[1] H.W. Kroto, J.R. Heath, S.C. O'Brien, R.F. Curl, R.E. Smalley, C_{60}: Buckminsterfullerene, Nature 318 (1985) 162–163.

[2] H. Murayama, S. Tomonoh, J.M. Alford, M.E. Karpuk, Fullerene production in tons and more: from science to industry, Fullerenes, Nanotubes, Carbon Nanostruct. 12 (2004) 1–9.

[3] Woodrow Wilson International Center for Scholars, The project on emerging nanotechnologies, http://www.nanotechproject.org/consumerproducts (2012).

[4] E. Oberdörster, S. Zhu, T.M. Blickley, P. McClellan-Green, M.L. Haasch, Ecotoxicology of carbon-based engineered nanoparticles: effects of fullerene (C_{60}) on aquatic organisms, Carbon 44 (2006) 1112–1120.

[5] C.W. Isaacson, M. Kleber, J.A. Field, Quantitative analysis of fullerene nanomaterials in environmental systems: a critical review, Environ. Sci. Technol. 43 (2009) 6463–6474.

[6] S. Kang, M.S. Mauter, M. Elimelech, Microbial cytotoxicity of carbon-based nanomaterials: implications for river water and wastewater effluent, Environ. Sci. Technol. 43 (2009) 2648–2653.

[7] C.T. Jafvert, P.P. Kulkarni, Buckminsterfullerene's (C_{60}) octanol-water partition coefficient (K_{ow}) and aqueous solubility, Environ. Sci. Technol. 42 (2008) 5945–5950.

[8] S. Deguchi, R.G. Alargova, K. Tsujii, Stable dispersions of fullerenes, C_{60} and C_{70}, in water. preparation and characterization, Langmuir 17 (2001) 6013–6017.

[9] J.D. Fortner, D.Y. Lyon, C.M. Sayes, A.M. Boyd, J.C. Falkner, E.M. Hotze, L.B. Alemany, Y.J. Tao, W. Guo, K.D. Ausman, V.L. Colvin, J.B. Hughes, C_{60} in water: nanocrystal formation and microbial response, Environ. Sci. Technol. 39 (2005) 4307–4316.

[10] Z. Chen, P. Westerhoff, P. Herckes, Quantification of C_{60} fullerene concentrations in water, Environ. Toxicol. Chem. 27 (2008) 1852–1859.

[11] X. Qu, Y.S. Hwang, P.J.J. Alvarez, D. Bouchard, Q. Li, UV irradiation and humic acid mediate aggregation of aqueous fullerene (nC_{60}) nanoparticles, Environ. Sci. Technol. 44 (2010) 7821–7826.

[12] D.Y. Lyon, L.K. Adams, J.C. Falkner, P.J.J. Alvarez, Antibacterial activity of fullerene water suspensions: effects of preparation method and particle size, Environ. Sci. Technol. 40 (2006) 4360–4366.

[13] H. Hyung, J.H. Kim, Dispersion of C_{60} in natural water and removal by conventional drinking water treatment processes, Water Res. 43 (2009) 2463–2470.

[14] Q. Li, B. Xie, Y.S. Hwang, Y. Xu, Kinetics of C_{60} fullerene dispersion in water enhanced by natural organic matter and sunlight, Environ. Sci. Technol. 43 (2009) 3574–3579.

[15] X. Ma, D. Bouchard, Formation of aqueous suspensions of fullerenes, Environ. Sci. Technol. 43 (2009) 330–336.

[16] T.M. Benn, P. Westerhoff, P. Herckes, Detection of fullerenes (C_{60} and C_{70}) in commercial cosmetics, Environ. Pollut. 159 (2011) 1334–1342.

[17] S.R. Chae, E.M. Hotze, Y. Xiao, J. Rose, M.R. Wiesner, Comparison of methods for fullerene detection and measurements of reactive oxygen production in cosmetic products, Environ. Eng. Sci. 27 (2010) 797–804.

[18] M. Farré, S. Pérez, K. Gajda-Schrantz, V. Osorio, L. Kantiani, A. Ginebreda, D. Barceló, First determination of C_{60} and C_{70} fullerenes and N-methylfulleropyrrolidine C_{60} on the suspended material of wastewater effluents by liquid chromatography hybrid quadrupole linear ion trap tandem mass spectrometry, J. Hydrol. 383 (2010) 44–51.

[19] K. Kümmerer, J. Menz, T. Schubert, W. Thielemans, Biodegradability of organic nanoparticles in the aqueous environment, Chemosphere 82 (2011) 1387–1392.

[20] N.B. Hartmann, I.M. Buendia, J. Bak, A. Baun, Degradability of aged aquatic suspensions of C_{60} nanoparticles, Environ. Pollut. 159 (2011) 3134–3137.

[21] Y. Wang, P. Westerhoff, K.D. Hristovski, Fate and biological effects of silver, titanium dioxide, and C_{60} (fullerene) nanomaterials during simulated wastewater treatment processes, J. Hazard. Mater. 201–202 (2012) 16–22.

[22] J.A. Brant, J. Labille, J.Y. Bottero, M.R. Wiesner, Characterizing the impact of preparation method on fullerene cluster structure and chemistry, Langmuir 22 (2006) 3878–3885.

[23] K.T. Kim, M.H. Jang, J.Y. Kim, S.D. Kim, Effect of preparation methods on toxicity of fullerene water suspensions to Japanese medaka embryos, Sci. Total Environ. 408 (2010) 5606–5612.

[24] C. Wang, C. Shang, P. Westerhoff, Quantification of fullerene aggregate nC_{60} in wastewater by high-performance liquid chromatography with UV-vis spectroscopic and mass spectrometric detection, Chemosphere 80 (2010) 334–339.

[25] Y. Yang, N. Nakada, R. Nakajima, C. Wang, H. Tanaka, Toxicity of aqueous fullerene nC_{60} to activated sludge: nitrification inhibition and Microtox test, J. Nanomater. 2012 (2012) 1–6.

[26] L. Nyberg, R.F. Turco, L. Nies, Assessing the impact of nanomaterials on anaerobic microbial communities, Environ. Sci. Technol. 42 (2008) 1938–1943.

[27] R.J. Hunter, Zeta potential in colloid science: principles and applications, Academic press, London, 1981.

[28] P.G. Smith, P. Coackley, A method for determining specific surface area of activated sludge by dye adsorption, Water Res. 17 (1983) 595–598.

[29] B.L. Sørensen, R.J. Wakeman, Filtration characterisation and specific surface area measurement of activated sludge by Rhodamine B adsorption, Water Res. 30 (1996) 115–121.

[30] J.L. Hu, X.W. He, C.R. Wang, J.W. Li, C.H. Zhang, Cadmium adsorption characteristic

382 of alkali modified sewage sludge, Bioresour. Technol. 121 (2012) 25–30.
383 [31] M. Rosenberg, Bacterial adherence to hydrocarbons: a useful technique for studying cell-
384 surface hydrophobicity, FEMS Microbiol. Lett. 22 (1984) 289–295.
385 [32] Z. Geng, E.R. Hall, A comparative study of fouling-related properties of sludge from
386 conventional and membrane enhanced biological phosphorus removal processes, Water
387 Res. 41 (2007) 4329–4338.
388 [33] APHA, Standard Methods for the examination of water and wastewater, American Public
389 Health Association, Washington, DC, USA, 20th edition, 1999.
390 [34] Y.S. Ho, G. McKay, The sorption of lead (II) ions on peat, Water Res. 33 (1999) 578–
391 584.
392 [35] Y.S. Ho, G. McKay, The kinetics of sorption of divalent metal ions onto sphagnum moss
393 peat, Water Res. 34 (2000) 735–742.
394 [36] Y.S Ho, G McKay, Pseudo-second order model for sorption processes, Process Biochem.
395 34 (1999) 451–465.
396 [37] O. Gulnaz, A. Kaya, S. Dincer, The reuse of dried activated sludge for adsorption of
397 reactive dye, J. Hazard. Mater. 134 (2006) 190–196.
398 [38] G.V. Andrievsky, V.K. Klochkov, A.B. Bordyuh, G.I. Dovbeshko, Comparative analysis
399 of two aqueous-colloidal solutions of C_{60} fullerene with help of FTIR reflectance and UV-
400 Vis spectroscopy, Chem. Phys. Lett. 364 (2002) 8–17.
401 [39] R. Chang, Physical chemistry for the chemical and biological sciences, University
402 Science Books, Sausalito, CA, USA, 2000.
403 [40] M. Clara, B. Strenn, E. Saracevic, N. Kreuzinger, Adsorption of bisphenol-A, 17β-
404 estradiole and 17α-ethinylestradiole to sewage sludge, Chemosphere 56(2004) 843–851.
405 [41] Y.X. Ren, K. Nakano, M. Nomura, N. Chiba, O. Nishimura, A thermodynamic analysis
406 on adsorption of estrogens in activated sludge process, Water Res. 41 (2007) 2341–2348.

[42] M. Basibuyuk, C.F. Forster, An examination of the adsorption characteristics of a basic dye (Maxilon Red BL-N) on to live activated sludge system, Process Biochem. 38 (2003) 1311–1316.

[43] W.H. Li, Q.Y. Yue, B.Y. Gao, Z.H. Ma, Y.J. Li, H.X. Zhao, Preparation and utilization of sludge-based activated carbon for the adsorption of dyes from aqueous solutions, Chem. Eng. J. 171 (2011) 320–327.

[44] W.M. Ibrahim, Biosorption of heavy metal ions from aqueous solution by red macroalgae, J. Hazard. Mater. 192 (2011)1827–1835.

[45] I. Langmuir, The adsorption of gases on plane surfaces of glass, mica and platinum, J. Am. Chem. Soc. 40 (1918) 1361–1403.

[46] K.R. Hall, L.C. Eagleton, A. Acrivos, T. Vermeulen, Pore- and solid-diffusion kinetics in fixed-bed adsorption under constant-pattern conditions, Ind. Eng. Chem. Fundamen. 5 (1966) 212–223.

[47] R. Jain, V.K. Gupta, S. Sikarwar, Adsorption and desorption studies on hazardous dye Naphthol Yellow S, J. Hazard. Mater. 182 (2010) 749–756.

[48] H. Freundlich, Concerning adsorption in solutions, Z. Phys. Chem. 57 (1906) 385–470.

[49] A. Günay, E. Arslankaya, İ. Tosun, Lead removal from aqueous solution by natural and pretreated clinoptilolite: adsorption equilibrium and kinetics, J. Hazard. Mater. 146 (2007) 362–371.

[50] J.J. Liu, X.C. Wang, B. Fan, Characteristics of PAHs adsorption on inorganic particles and activated sludge in domestic wastewater treatment, Bioresour. Technol. 102 (2011) 5305–5311.

[51] D. Ding, Y. Zhao, S. Yang, W. Shi, Z. Zhang, Z. Lei, Y. Yang, Adsorption of cesium from aqueous solution using agricultural residue-Walnut shell: equilibrium, kinetic and thermodynamic modeling studies, Water Res. 2013, doi: org/10.1016/j.watres.2013.02.

014.

[52] C. Li, Y. Li, J. Wang, J. Cheng, PA6@Fe_xO_y nanofibrous membrane preparation and its strong Cr (VI)-removal performance, Chem. Eng. J. 220 (2013) 294–301.

[53] Y. Wang, Y. Mu, Q.B. Zhao, H.Q. Yu, Isotherms, kinetics and thermodynamics of dye biosorption by anaerobic sludge, Sep. Purif. Technol. 50 (2006) 1–7.

[54] Y. Xiao, M.R. Wiesner, Characterization of surface hydrophobicity of engineered nanoparticles, J. Hazard. Mater. 215–216 (2012) 146–151.

[55] Y. Yang, N. Nakada, R. Nakajima, M. Yasojima, C. Wang, H. Tanaka, pH, ionic strength and dissolved organic matter alter aggregation of fullerene C_{60} nanoparticles suspensions in wastewater, J. Hazard. Mater. 244-245 (2012) 582–587.

[56] Z. Reddad, C. Gerente, Y. Andres, P. Le Cloirec, Adsorption of several metal ions onto a low-cost biosorbent: kinetic and equilibrium studies, Environ. Sci. Technol. 36 (2002) 2067–2073.

[57] Z. Aksu, A.B. Akın, Comparison of Remazol Black B biosorptive properties of live and treated activated sludge, Chem. Eng. J. 165 (2010) 184–193.

[58] Q. Zhou, S. Deng, Q. Zhang, Q. Fan, J. Huang, G. Yu, Sorption of perfluorooctane sulfonate and perfluorooctanoate on activated sludge, Chemosphere 81 (2010) 453–458.

[59] M.A. Kiser, D.A. Ladner, K.D. Hristovski, P.K. Westerhoff, Nanomaterial transformation and association with fresh and freeze-dried wastewater activated sludge: implications for testing protocol and environmental fate, Environ. Sci. Technol. 46 (2012) 7046–7053.

List of Table captions

Table 1 − Experimental conditions for the studies of influencing factors.

Table 2 − Calculated parameters of adsorption kinetics models.

Table 3 − Calculated parameters of adsorption isotherm models.

List of Figure captions

Fig. 1 – Time profile of nC_{60} adsorption on activated sludge.

Fig. 2 – Adsorption kinetics of nC_{60} on activated sludge by (a) pseudo-first-order model and (b) pseudo-second-order model.

Fig. 3 – (a) Langmuir and (b) Freundlich adsorption isotherms of nC_{60} on activated sludge.

Fig. 4 – nC_{60} adsorption on activated sludge as a function of (a) MLSS and (b) temperature. C_0: the initial nC_{60} concentration in aqueous phase; C: the nC_{60} concentration in aqueous phase after 1-h mixture.

Fig. 5 – nC_{60} adsorption on activated sludge as a function of (a) ionic strength, (b) pH, and (c) wastewater DOM. C_0: the initial nC_{60} concentration in aqueous phase; C: the nC_{60} concentration in aqueous phase after 1-h mixture.

Fig. 6 − ζ potential of activated sludge in wastewater and concentration of dissolved organic carbon (DOC) in supernatant in sludge mixture (without nC_{60}) as a function of (a) ionic strength, (b) pH, and (c) wastewater DOM.

476 # List of Figure caption in Supplementary data

477 **Fig. S1** – (a) Intensity-weighted size distribution of nC_{60} in Milli-Q water (pH=5.6, *T*=25 °C).

478 (b) ζ potential of nC_{60} in Milli-Q water as a function of pH (*T*=25 °C).

479 (c) ζ potential of nC_{60} in three wastewater samples (pH=7, *T*=25 °C).

480

481

Table 1

Experimental conditions for the studies of influencing factors.

Experiments	Wastewater	nC_{60} (mg/L)	Temperature (°C)	MLSS (mg/L)	pH	Added ionic strength (mM NaCl)	Contact time (h)
MLSS	PE	0.200	25	50–4000	7	not adjusted	1
Temperature			15–35	1000	7	not adjusted	
Ionic strength			25	1000	7	0–500	
pH			25	1000	3–11	not adjusted	
Wastewater DOM	PE, AT, SE	0.200	25	1000	7	not adjusted	1

PE: primary effluent; AT: aeration tank liquor; SE: secondary effluent

Table 2

Calculated parameters of adsorption kinetics models.

Concentration (mg/L)	$q_{e(obs)}$ (mg/g)	Pseudo-first-order model			Pseudo-second-order model		
		k_1 (1/h)	$q_{e(cal)}$ (mg/g)	R^2	k_2 (g/(mg·h))	$q_{e(cal)}$ (mg/g)	R^2
0.100	0.074	0.225	0.030	0.641	48.310	0.072	0.998
0.300	0.230	0.299	0.104	0.826	11.913	0.237	0.998
0.500	0.380	0.286	0.233	0.938	4.124	0.386	0.995

Table 3

Calculated parameters of adsorption isotherm models.

Langmuir model				Freundlich model		
k_L (L/mg)	q_m (mg/g)	R_L	R^2	k_F	n	R^2
3.147	1.949	0.389	0.966	4.221	1.081	0.999

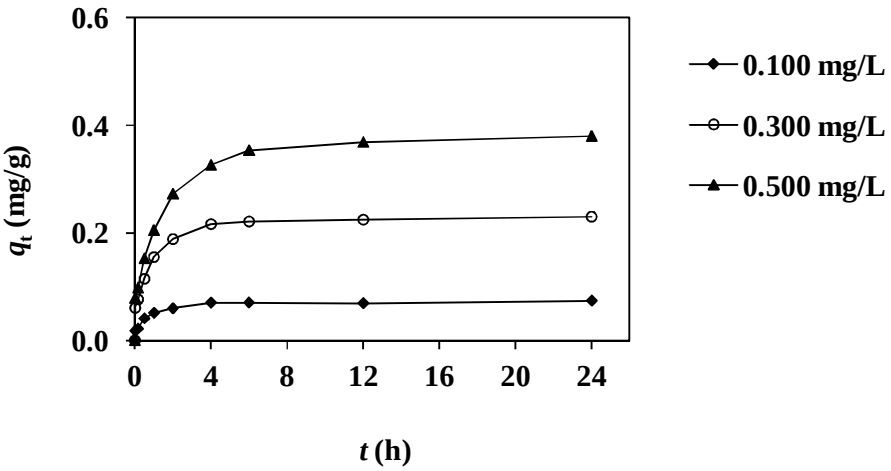

Fig. 1 − Time profile of nC_{60} adsorption on activated sludge.

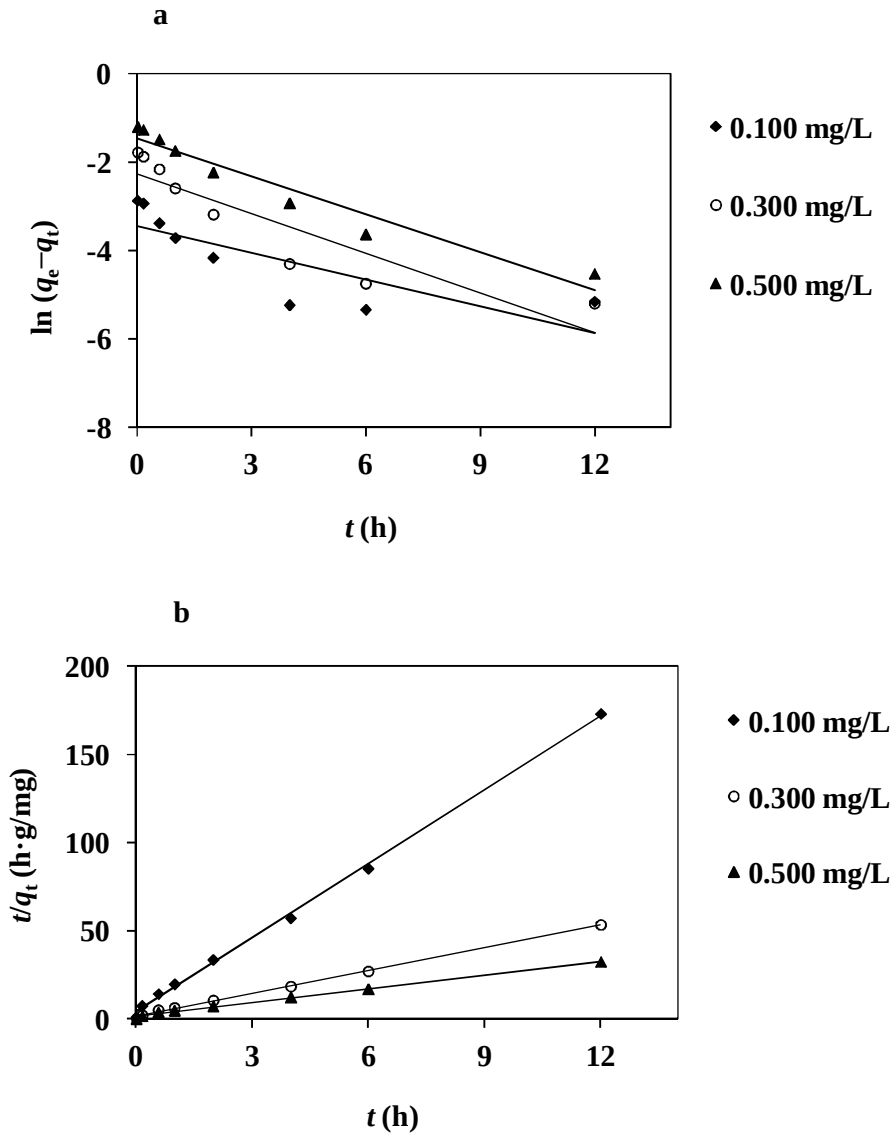

Fig. 2 − Adsorption kinetics of nC_{60} on activated sludge by (a) pseudo-first-order model and (b) pseudo-second-order model.

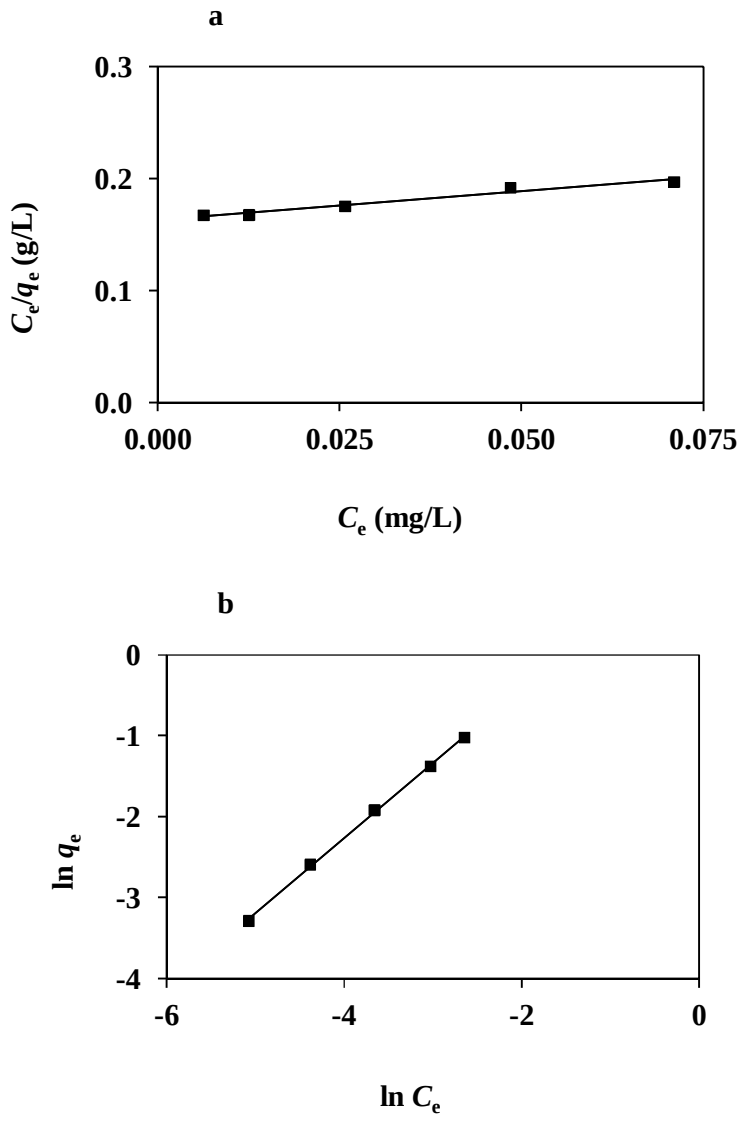

Fig. 3 − (a) Langmuir and (b) Freundlich adsorption isotherms of nC_{60} on activated sludge.

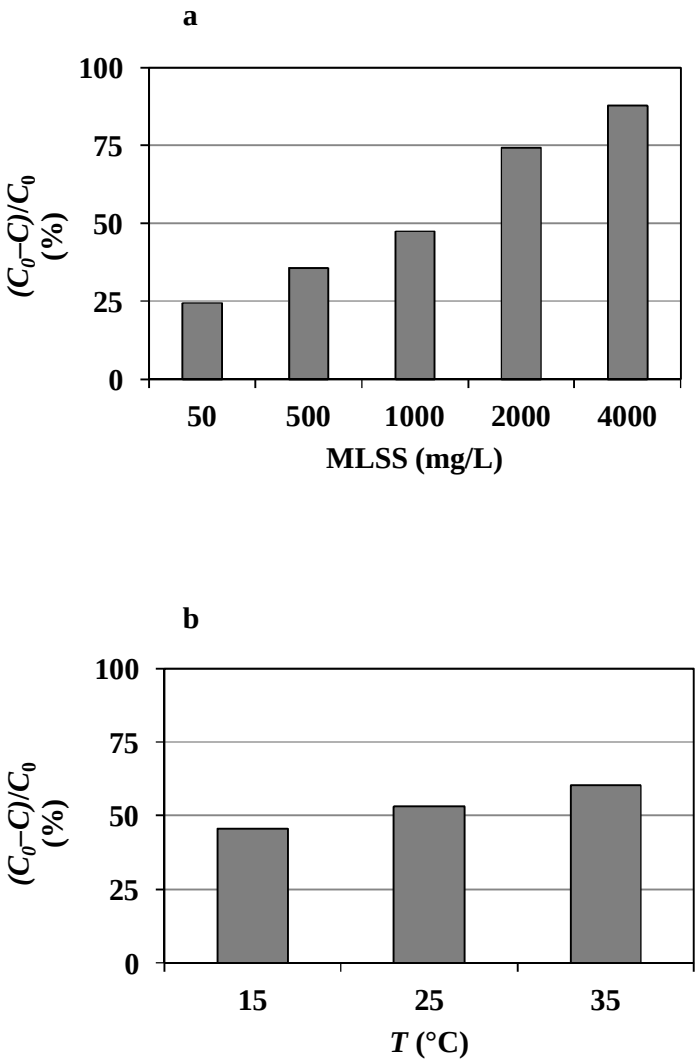

Fig. 4 − nC_{60} adsorption on activated sludge as a function of (a) MLSS and (b) temperature. C_0: the initial nC_{60} concentration in aqueous phase; C: the nC_{60} concentration in aqueous phase after 1-h mixture.

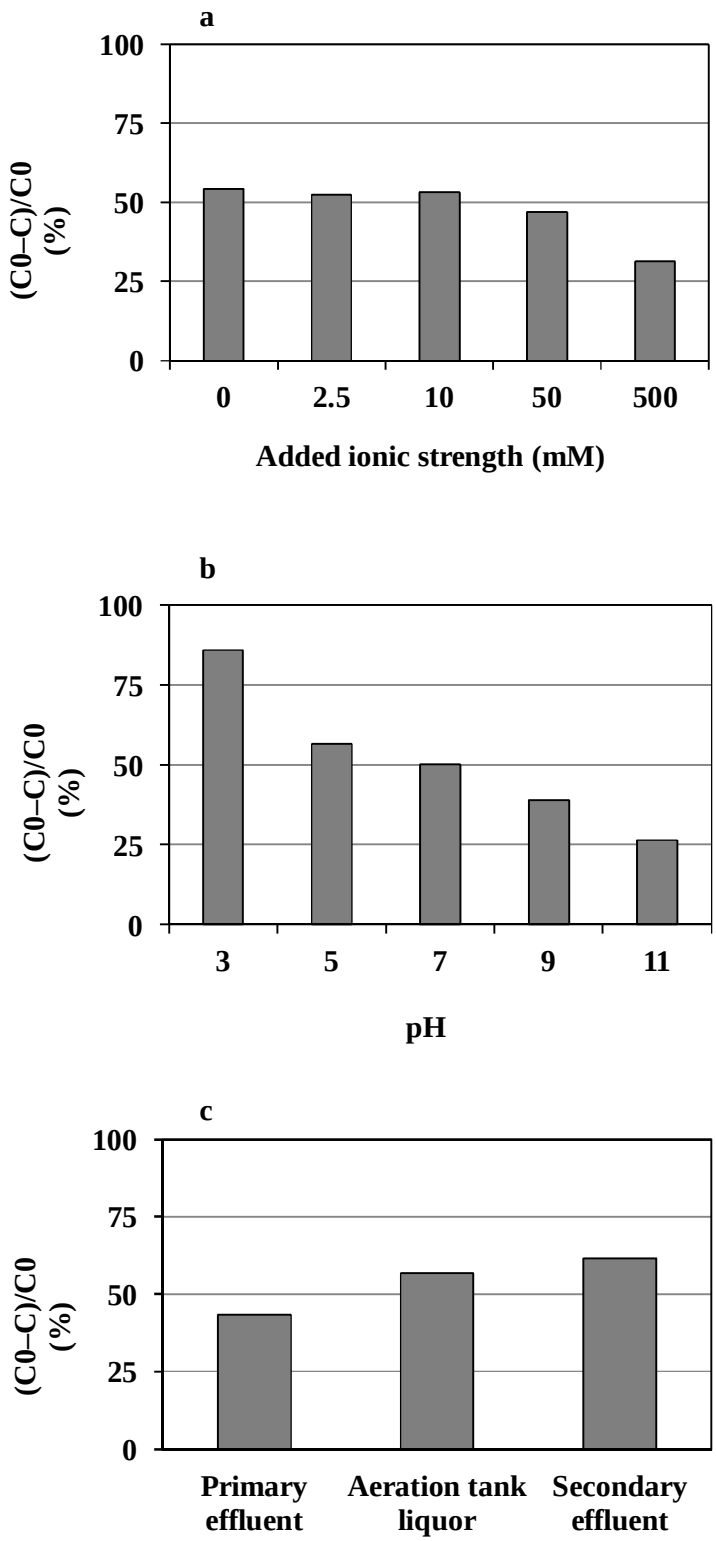

Fig. 5– nC_{60} adsorption on activated sludge as a function of (a) ionic strength, (b) pH, and (c) wastewater DOM. C_0: the initial nC_{60} concentration in aqueous phase; C: the nC_{60} concentration in aqueous phase after 1-h mixture.

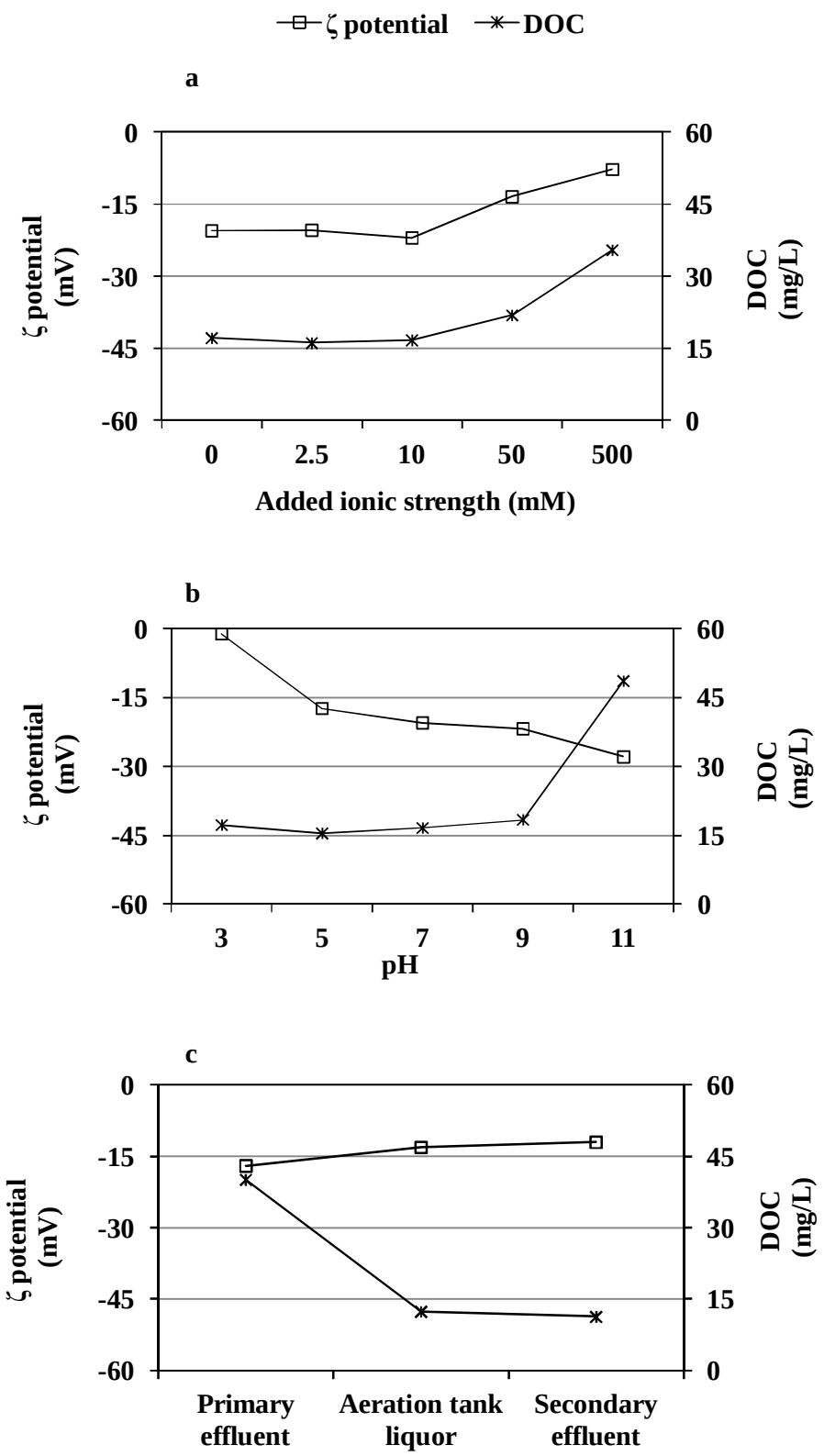

Fig. 6 − ζ potential of activated sludge in wastewater and concentration of dissolved organic carbon (DOC) in supernatant in sludge mixture (without nC_{60}) as a function of (a) ionic strength, (b) pH, and (c) wastewater DOM.